

Relation between 2D/3D chirality and the appearance of chiroptical effects in real nanostructures

Oriol Arteaga,^{1,*} Jordi Sancho-Parramon,² Shane Nichols,³
Ben M. Maoz,⁴ Adolf Canillas,¹ Salvador Bosch,¹ Gil Markovich,⁴
and Bart Kahr³

¹*Dep. Física Aplicada i Òptica, C/ Martí i Franquès, Universitat de Barcelona, 08030, Barcelona, Spain*

²*Rudjer Boskovic Institute, Bijenička 54, 10000, Zagreb, Croatia*

³*Dep. of Chemistry, 100 Washington Square East, Room 1001, New York University, New York, New York 10003, USA*

⁴*Dep. of Chemical Physics, School of Chemistry, Raymond and Beverly Sackler Faculty of Exact Sciences, Tel Aviv University, Tel Aviv, 69978 Israel*

[*oartega@edu](mailto:oartega@edu)

Abstract: The optical activity of fabricated metallic nanostructures is investigated by complete polarimetry. While lattices decorated with nanoscale gammadia etched in thin metallic films have been described as two dimensional, planar nanostructures, they are better described as quasi-planar structures with some three dimensional character. We find that the optical activity of these structures arises not only from the dissymmetric backing by a substrate but, more importantly, from the selective rounding of the nanostructure edges. A true chiroptical response in the far-field is only allowed when the gammadia contain these non-planar features. This is demonstrated by polarimetric measurements in conjunction with electrodynamic simulations based on the discrete dipole approximation that consider non-ideal gammadia. It is also shown that subtle planar dissymmetries in gammadia are sufficient to generate asymmetric transmission of circular polarized light.

© 2016 Optical Society of America

OCIS codes: (160.4236) Nanomaterials; (160.1585) Chiral media; (240.6680) Surface plasmons.

References and links

1. A. Papakostas, A. Potts, D. M. Bagnall, S. L. Prosvirnin, H. J. Coles, and N. I. Zheludev, "Optical manifestations of planar chirality," *Phys. Rev. Lett.* **90**, 107404 (2003).
2. W. Zhang, A. Potts, and D. M. Bagnall, "Giant optical activity in dielectric planar metamaterials with two-dimensional chirality," *J. Opt. A: Pure Appl. Opt.* **8**, 878–890 (2006).
3. K. Jefimovs, N. Saito, Y. Ino, T. Vallius, P. Vahimaa, J. Turunen, R. Shimano, M. Kauranen, Y. Svirko, and M. Kuwata-Gonokami, "Optical activity in chiral gold nanogratings," *Microelectron. Eng.* **78-79**, 448–451 (2005).
4. E. Hendry, T. Carpy, J. Johnston, M. Popland, R. V. Mikhaylovskiy, A. J. Laphorn, S. M. Kelly, L. D. Barron, N. Gadegaard, and M. Kadodwala, "Ultrasensitive detection and characterization of biomolecules using super-chiral fields," *Nat. Nanotechnol.* **5**, 783–787 (2010).
5. A. Ben-Moshe, B. M. Maoz, A. O. Govorov, and G. Markovich, "Chirality and chiroptical effects in inorganic nanocrystal systems with plasmon and exciton resonances," *Chem. Soc. Rev.* **42**, 7028–7041 (2013).

6. Y. J. Liu, S. Wu, D. Popp, E. S. P. Leong, Y. L. Hor, W. K. Phua, K. L. Mok, J. H. Teng, R. Robinson, E. P. Li, and E. H. Khoo, "Effect of asymmetrical nanostructures on detecting the optical rotational properties of large biofilament structures," *Proc. SPIE*, **8809**, 88090D (2013).
7. K. Konishi, B. Bai, X. Meng, P. Karvinen, J. Turunen, Y. P. Svirko, and M. Kuwata-Gonokami, "Observation of extraordinary optical activity in planar chiral photonic crystals," *Opt. Express* **16**, 7189–7196 (2008).
8. M. Schäferling, D. Dregely, M. Hentschel, and H. Giessen, "Tailoring enhanced optical chirality: design principles for chiral plasmonic nanostructures," *Phys. Rev. X* **2**, 031010 (2012).
9. T. Cao, L. Zhang, R. E. Simpson, C. Wei, and M. J. Cryan, "Strongly tunable circular dichroism in gammadion chiral phase-change metamaterials," *Opt. Express* **21**, 27841–27851 (2013).
10. N. Kanda, K. Konishi, and M. Kuwata-Gonokami, "Light-induced terahertz optical activity," *Opt. Lett.* **34**, 3000–3002 (2009).
11. D.-H. Kwon, P. L. Werner, and D. H. Werner, "Optical planar chiral metamaterial designs for strong circular dichroism and polarization rotation," *Opt. Express* **16**, 11802–11807 (2008).
12. B. Bai, Y. Svirko, J. Turunen, and T. Vallius, "Optical activity in planar chiral metamaterials: theoretical study," *Phys. Rev. A* **76**, 023811 (2007).
13. M. Kuwata-Gonokami, N. Saito, Y. Ino, M. Kauranen, K. Jefimovs, T. Vallius, J. Turunen, and X. Luo, "Giant optical activity in quasi-two-dimensional planar nanostructures," *Phys. Rev. Lett.* **95**, 227401 (2005).
14. E. Plum, V. A. Fedotov, and N. I. Zheludev, "Asymmetric transmission: a generic property of two-dimensional periodic patterns," *J. Opt.* **13**, 024006 (2011).
15. V. A. Fedotov, A. S. Schwanecke, N. I. Zheludev, V. V. Khardikov, and S. L. Prosvirnin, "Asymmetric transmission of light and enantiomerically sensitive plasmon resonance in planar chiral nanostructures," *Nano Lett.* **7**, 1996–1999 (2007).
16. V. A. Fedotov, P. L. Mladyonov, S. L. Prosvirnin, A. V. Rogacheva, Y. Chen, and N.I. Zheludev, "Asymmetric propagation of electromagnetic waves through a planar chiral structure," *Phys. Rev. Lett.* **97**, 167401 (2006).
17. Z. Li, M. Gokkavas, and E. Ozbay, "Manipulation of asymmetric transmission in planar chiral nanostructures by anisotropic loss," *Adv. Opt. Mat.* **1**, 482–488 (2013).
18. X. Ma, C. Huang, M. Pu, Y. Wang, Z. Zhao, C. Wang, and X. Luo, "Dual-band asymmetry chiral metamaterial based on planar spiral structure," *Appl. Phys. Lett.* **101**, 161901 (2012).
19. O. Arteaga, J. Freudenthal, B. Wang, and B. Kahr, "Mueller matrix polarimetry with four photoelastic modulators: theory and calibration," *Appl. Opt.* **51**, 6805–6817 (2012).
20. O. Arteaga and A. Canillas, "Analytic inversion of the Mueller-Jones polarization matrices for homogeneous media," *Opt. Lett.* **35**, 559–561 (2010).
21. R. Ossivokski, "Differential matrix formalism for depolarizing anisotropic media," *Opt. Lett.* **36**, 2330–2332 (2011).
22. O. Arteaga and B. Kahr, "Characterization of homogenous depolarizing media based on Mueller matrix differential decomposition," *Opt. Lett.* **38**, 1134–1136 (2013).
23. O. Arteaga, "Mueller matrix polarimetry of anisotropic chiral media," Phd Thesis, Universitat de Barcelona (2010).
24. O. Arteaga, "A note on optical activity and extrinsic chirality," **2015**, <http://arxiv.org/abs/1508.02422>.
25. B. T. Draine and P. J. Flatau, "Discrete-dipole approximation for scattering calculations," *J. Opt. Soc. Am. A* **11**, 1491–1499 (1994).
26. B. T. Draine and P. J. Flatau, "Discrete-dipole approximation for periodic targets: theory and tests," *J. Opt. Soc. Am. A* **25**, 2693–2703 (2008).
27. O. Arteaga, B. M. Maoz, S. Nichols, G. Markovich, and B. Kahr, "Complete polarimetry on the asymmetric transmission through subwavelength hole arrays," *Opt. Express* **22**, 13719–13732 (2014).
28. O. Arteaga, "Number of independent parameters in the Mueller matrix representation of homogeneous depolarizing media," *Opt. Lett.* **38**, 1131–1133 (2013).
29. S.I. Maslovski, D. K. Morits, and S. A. Tretyakov, "Symmetry and reciprocity constraints on diffraction by gratings of quasi-planar particles," *J. Opt. A: Pure Appl. Opt.* **11**, 074004 (2009).

1. Introduction

A gammadion is a bent-arm, decorative symbol with fourfold symmetry. As a repeating design element in nanostructured arrays, metallic gammadions with features smaller than the wavelength of light have been reported to exhibit large chiroptical effects [1–3] and/or to amplify optical activity from biopolymer analytes [4–6]. Arrays of gammadion-shaped nanostructures have been used to engineer devices based on the large associated optical activities and polarization conversions [1–3, 7–12].

Gammadions have frequently been characterized as "2D chiral" structures. A 2D chiral object (Fig. 1) is a pattern that cannot be brought into congruence with its mirror image unless it is

lifted from the plane. The sense of twist of a 2D chiral structure changes depending on the side from which is observed. A 3D chiral object keeps the same handedness even if the object is turned around. Optical activity is a reciprocal property (e.g. it obeys the Lorentz reciprocity principle), which means that it should not change when reversing the light path through the medium. Therefore optical activity can never be a direct consequence of geometric 2D chirality.



Fig. 1. Pictorial comparison between 2D and 3D chirality. An object (that is not necessarily 2D) is “2D chiral” when it can be brought into congruence with its mirror image when it is lifted from the plane.

Optical activity in gammadia arrays was first observed experimentally by Kuwata-Gonokami et al [13]. It was justified by some three dimensionality in the structures induced by the substrate, i.e. from the asymmetry of light-plasmon coupling at the air-metal and substrate-metal interfaces. Nevertheless, several subsequent publications [2, 14–18] have also reported the asymmetric transmission for circular polarization in planar structures, meaning that opposite sides of the sample transmit circular polarization in different amounts (i.e. non-reciprocal response). There seems to exist some confusion in the literature of planar metamaterials because there coexist reciprocal and non-reciprocal observations, and the structural features that permit optical activity or asymmetric transmission do not seem to be well understood.

In this work we analyze the interaction of metallic nanostructured planar gammadia with polarized light to understand the structural features that give rise to optical activity and to distinguish them from those that induce asymmetric transmission of circularly polarized light (CPL). In section 2, we investigate the optical response of nanofabricated gammadia with complete transmission polarimetry. Electrodynamical simulations are presented in section 3 that account for the dissymmetries of real metallic gammadia introduced in manufacture, and from which it is shown that reciprocal optical activity and/or asymmetric transmission of circular polarized light can arise.

2. Experiments

Here, we consider light transmission at normal incidence through square arrays of gold gammadia. The optical response is analyzed in the far field for all possible polarization states in terms of the Mueller matrix (\mathbf{M}).

Two square arrays of gold nanostructures were fabricated using electron beam lithography, one with left-handed gammadia and the other with right-handed gammadia. Each array occupies $400 \times 400 \mu\text{m}^2$ and each gammadion is inscribed in a $500 \times 500 \text{nm}^2$ square. The gaps between neighboring gammadia measure 100 nm. The thickness of each gammadion is 75 nm. A 5 nm layer of Cr was added to the glass substrate to improve the adhesion of gold. Scanning electron microscopy (SEM) micrographs are shown in Fig. 2.

The optical responses of the gammadia were studied with a spectroscopic Mueller matrix polarimeter [19] in the range 350-800 nm. This instrument uses four photoelastic modulators (Hinds Instruments) simultaneously operating at different frequencies, two in the polarization state generator and two in the polarization state analyzer. The fifteen elements of a normal-

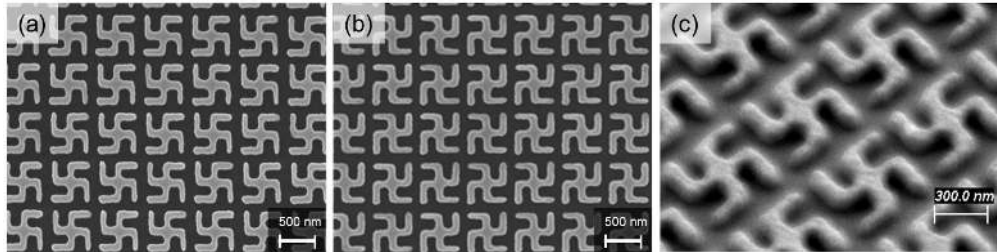


Fig. 2. Scanning electron micrographs of gold gammadia. Panels (a) and (b) show a top view of the left- and right-handed arrays, while panel (c) shows a detail of the 3D character of the gammadia not evident from the top views.

ized Mueller matrix were measured without moving any optical component. All measurements were in transmission at normal incidence using an effective light spot of around $250 \mu\text{m}$. No depolarization was observed. The experiments were repeated by turning the backside of the samples towards the light source, thus effectively changing the sign of the wave vector. In the first pass, light was incident on the gold gammadia (forward configuration) and in the second pass, light entered the sample through the glass substrate (backward configuration). We calculated the circular dichroism (CD) and circular birefringence (CB) from the Mueller matrix using the analytic inversion method [20] which, in absence of depolarization, provides the same results as the differential Mueller matrix decomposition [21, 22].

Sometimes the term “optical activity” is used to designate only the CB property but, more generally, it involves both CD and/or CB. The calculation of CD and CB from the Mueller matrix is a rigorous approach for the determination of the optical activity of linear anisotropic materials [20, 23]. Simpler experimental approaches sometimes used to determine CD, such as alternating illumination with left and right circularly polarized light (which is equivalent to measuring only the Mueller matrix element m_{03}), can give misleading results because the circular polarization is not preserved along the pathlength due to the effect of linear dichroism and linear birefringence [24].

Figure 3 shows the CD and CB spectra for the two 2D enantiomorphous (mirror image) gammadia arrays. As anticipated, CD and CB are approximately the same for forward and backward propagation, since optical activity is a reciprocal phenomenon. This is *always* true, even if for backward propagation the light beam approaches to gammadia that appear as mirror images of those seen in forward propagation. Therefore, the optical activity must arise due to mirror breaking dissymmetries that can not be altered by reversing the sign of the wave vector. Of course, our left- and right-handed arrays [Figs. 2(a) and 2(b)] whose sense is defined when looking at the substrate, not through it, still show CD and CB spectra of opposite sign. Such samples are true 3D enantiomorphs. The structural dissymmetries that generate this 3D chirality will be discussed in the next section.

3. Simulations

Simulations have been performed using the open-source DDSCAT code [25], which is an implementation of the discrete dipole approximation method (DDA) to calculate the scattering and absorption of electromagnetic waves by targets given by collections of polarizable point dipoles. DDA is flexible regarding the shape and size of targets, so our targets consist of arrays of dipoles that approximate various gold gammadia geometries. DDSCAT is able to describe the far-field scattering properties of a target in terms of the 2×2 scattering amplitude matrix or the Mueller matrix and it can deal with finite or periodic targets [26]. In all our simulations the

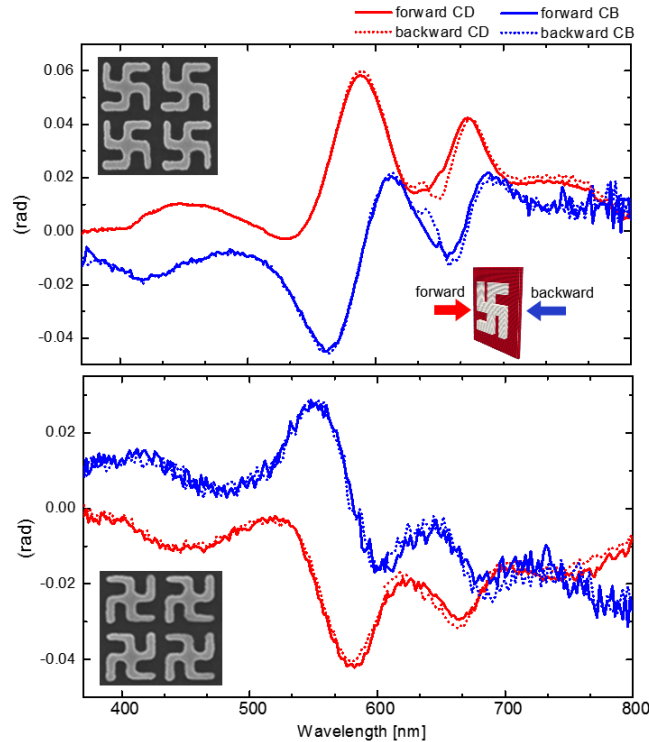


Fig. 3. The measured CD and CB spectra of the two gammadia samples with opposite handedness in the forward and backward configurations.

ambient refractive index was taken as 1.25 (a value between the refractive index of air and of the SiO₂ substrate). The main resonance of our ~ 500 nm gold gammadia is in the infrared, at around 2000 nm [Fig. 4(a)]. In our experiments, we have mostly studied the third resonance that falls at around 600 nm. The resonance at 2000 nm corresponds to a dipolar-like mode in which positive and negative surface charges are distributed on opposite sides of the gammadion as a function of the polarization by the incoming radiation [Fig. 4(b)]. Resonances at higher energies correspond to higher order multipole modes.

We simulated the Mueller matrix of gammadia perturbed by structural non-idealities or by a bounding surface. First we simulated an ideal gammadion, a planar, centrosymmetric nanostructure with four-fold rotational symmetry surrounded by the ambient medium on both sides. The simulated Mueller matrix for such a gammadion [Fig. 5(a)] is the identity matrix, which means that there is perfect polarization preservation between the input and output beams. This is the expected result for a structure with $4/m$ symmetry. Of course this confirms the fundamental idea that can be derived from symmetry arguments: *an ideal gammadion cannot possess any optical activity by itself*. Next, we simulated a gammadion with one of the four arms narrower than the others. This breaks the four-fold symmetry but preserves the perpendicular mirror. This perturbed gammadion modifies the polarization of transmitted light according to the Mueller matrix given in Fig. 5(b). This structure allows the asymmetric transmission of CPL due to the coupling of misaligned two-fold symmetric plasmonic modes [27]; the sense of this misalignment changes when the sample is turned over. This optical response, not to be confused with optical activity, is typically recognized by Mueller matrix elements M_{03} and M_{30} that are equal in absolute magnitude but opposite in sign, while elements M_{12} and M_{21} remain equal. Here,

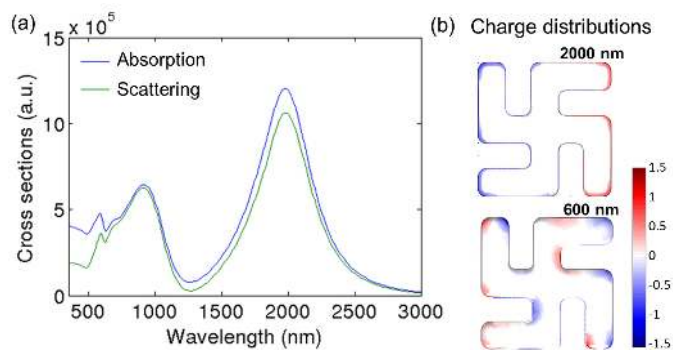


Fig. 4. (a) Spectroscopic simulation of the scattering and absorption cross-section of the $500 \times 500 \text{ nm}^2$ the gammadion nanostructure. (b) Surface charge density on the nanostructures at an arbitrary time point. This corresponds to excitation with horizontal linear polarization.

CD=0 and CB=0. The non-reciprocity is not related in any way to the optical activity [27, 28].

Finally, we simulated gammadia with characteristics that break the mirror symmetry with respect to the plane parallel to the sample surface, i.e. the perpendicular mirror plane. Two perturbations that occur in almost any nanofabricated structure were considered: the existence of a substrate or adhesion layer and the rounded, rather than sharp, edges of the structures. In the first simulation [Fig. 5(c)], we considered an extra Cr adhesion layer (the thick SiO_2 substrate was not simulated because it cannot be efficiently discretized in point dipoles). Surface plasmon resonances are very sensitive to small material changes, and the Cr layer under a gammadion generates a true 3D enantiomorph. Substrates or layers made of isotropic materials typically have no influence on normal-incidence polarimetric measurements, but for 2D chiral plasmonic nanostructures it provides the means for magnetoelectric interactions that generate optical activity. The effect of a dielectric substrate on the optical activity for arrays of plasmonic 2D structures was experimentally shown in [13] theoretically studied in [29]. Any 2D chiral object deposited on a substrate is susceptible to induce optical activity but, probably, only when surface plasmons are involved magnetoelectric interactions are large enough to produce detectable chiroptical signals.

In the second simulation [Fig. 5(d)] we considered a gammadion with rounded edges that mimics the shape observed in the SEM micrograph [Fig. 2(c)]. This was achieved by thinning the arms of the gammadion (i.e. reducing the number of dipoles) as the top surface is approached. In Figs. 5(c) and 5(d) the presence of optical activity is manifested by the symmetries $M_{03} = M_{30}$ and $M_{12} = -M_{21}$ in the Mueller matrix elements that, in absence of other linear effects, are respectively responsible for CD and CB.

In general, the more rounded the edges the greater the chiroptical effects because the nanostructure becomes less planar. Similarly, the more distinct refractive indices between the ambient medium and the substrate, the greater the optical activity. According to realistic simulations of our nanostructures, with the rounding affecting the upper 40 nm of the nanostructure and taking into account the spectroscopic refractive index of Cr (e.g. $n=3.13$ and $k=4.26$ at 600 nm), the overall contribution of the rounded edges to optical activity tends to be slightly greater than the effect of the Cr layer. It is also interesting to realize that the complete polarimetric response of the gammadia in Figs. 5(c) and 5(d) is reciprocal (because of the symmetries $M_{03} = M_{30}$ and $M_{12} = -M_{21}$, as it was discussed in Ref. [28]), i.e. it remains unaltered if the sample is turned over, unlike in Figs. 5(b). However, if the sense of the gammadia is reversed by a reflection

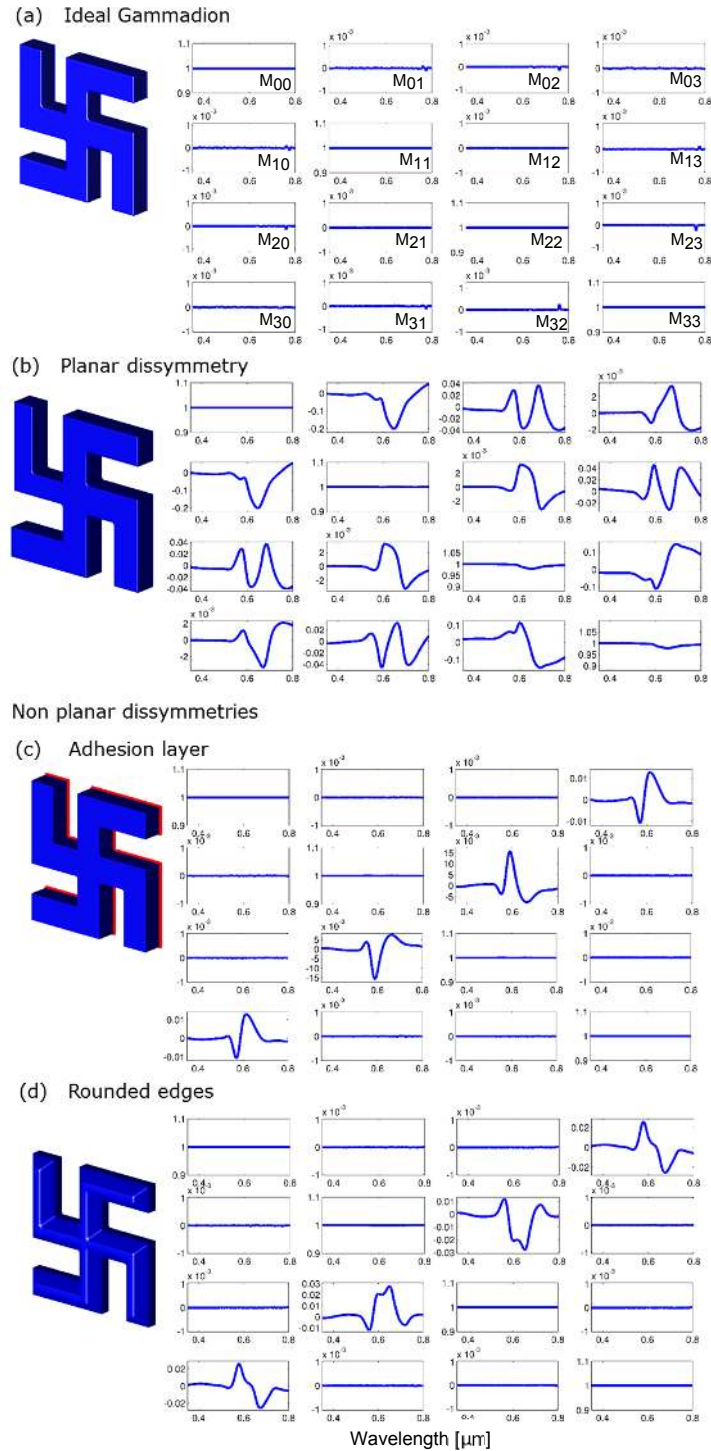


Fig. 5. Simulated Mueller matrices for four different types of gammadion nanostructures: an ideal gammadion with 4/m symmetry (a), a planar gammadion with one of the four arms narrowed (b) and two non-planar gammadia due to a substrate (c) or rounded edges (d).

operation, the 3D handedness of the non-ideal structure is also reversed, and CB and CD must change sign. Even though the sense of the gammadia is *apparently* reversed by a proper rotation, when examination is made through the back side, the sign of CB and CD are and must be preserved as for proper rotations of any chiral object in real space.

Table 1. Summary of optical effects in gammadia.

Type of sample	CD/CB	Asym. CPL
Ideal gammadia	No	No
Gammadia with planar dissymmetry ^a	No	Yes
Gammadia with non-planar dissymmetry ^b	Yes	No

^a A planar dissymmetry preserves the perpendicular mirror plane but breaks the four-fold symmetry.

^b A non-planar dissymmetry breaks the perpendicular mirror plane symmetry.

Table 1 summarizes the optical effects in the three classes of gammadia we have simulated. Both, optical activity (manifested as CD and CB) and asymmetric transmission of CPL, arise as a differential response of the gammadia to the handedness of the incoming polarization, but only optical activity is reciprocal and is strictly forbidden in planar structures. The asymmetric transmission of CPL is not an elementary optical effect of the structure, but is a consequence of the joint contribution of the linear birefringence (LB) and linear dichroism (LD) of two distinct two-fold symmetric plasmonic resonant modes. It cannot survive in absence of these linear anisotropies.

4. Discussion

Our fabricated gammadia are affected by each of the non-idealities listed in Fig. 5. A closer observation of Figs. 2(a) and 2(b) reveals that one of the central gammadion arms is thicker than the others. At the same time, Fig. 2(c) shows that the gammadia are non-planar due to rounded edges furthest from the substrate; moreover, the gammadia are written on top of a substrate that damps the optical response on one side. The presumption that these effects have small optical consequences, and that gammadia can be taken as $4/m$ idealities, is not supported by our simulations. We think that some of the contradictory and eventually confusing reports about optical activity in “apparently planar” gammadia are consequences of the failure to account for dissymmetries in manufacture.

More realistic simulations must include all the perturbations listed in Fig. 5 and, additionally, they would treat gammadia in arrays, not an individual gammadion. An experimental Mueller matrix measurement is shown in Fig. 6(a) together with simulations corresponding to a realistic isolated gammadion and a realistic gammadia array [Fig. 6(b)]. Coupling between neighbors clearly modifies the complexity of the polarimetric response. The agreement between experiment and simulations is only qualitative, but certain Mueller matrix elements are quite well reproduced. Due to the resonant nature of plasmonic peaks seen in the graphs, subtle variations in the gold nanostructures lead to remarkably different simulations. It is hard to quantify the degree of edge rounding from SEM micrographs, but some edges are smoother than others, and these differences were not embodied in the simulations. Additionally, the lithographic process shows some heterogeneity across the patterned area and, for example, there is some surface roughness that is difficult to see with SEM. This roughness is a source of localized surface plasmons that probably broaden the response. Another substantial difference between experiments and simulations is that simulations only take into account the thin Cr adhesion layer, but not the thick SiO₂ substrate.

Given the limitations of current nanofabrication techniques, it is realistic to presume that the fabrication of truly planar nanostructures will remain a challenge. Our gammadia are only

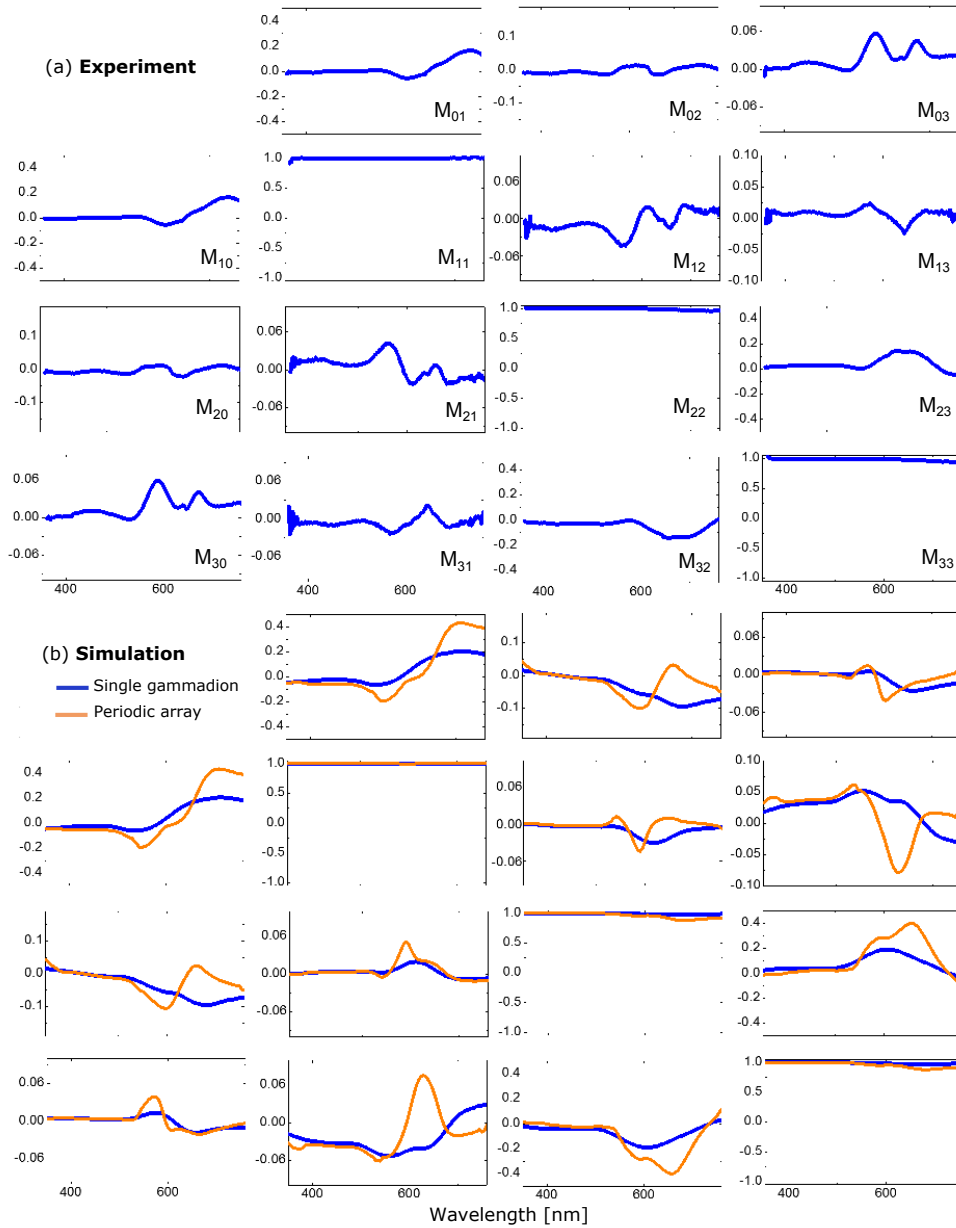


Fig. 6. Comparison of an experimental Mueller matrix measurement in the gammadion array (a) with two simulations (b). The same scale is used for both plots. The simulation in blue corresponds to a single realistic gammadion with narrowed vertical arms, rounded top edges, and backed by a thin Cr layer. The simulation in orange corresponds to a square array of gammadia with each gammadion having the same characteristic as that isolated but spaced by 100 nm from neighbors. All Mueller matrices have been normalized to their element M_{00} .

quasi-planar; while at first glance they appear to be mirror symmetric, they are in fact decidedly enantiomorphous in 3D. Even small structural perturbations easily overlooked can generate remarkably high values of CD and CB. Gammadia are susceptible to ordinary, reciprocal gyration whenever the plane symmetry is broken and this is the lithographic norm.

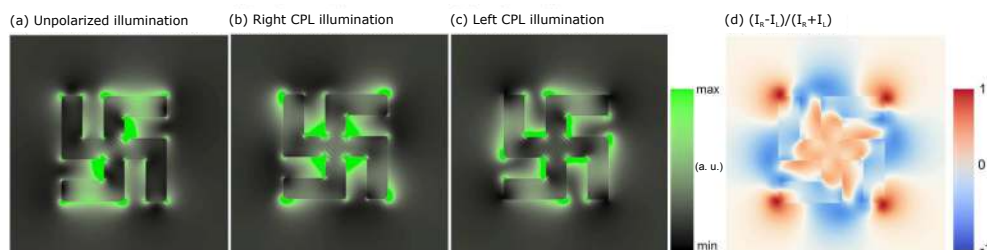


Fig. 7. Calculated electric field intensities at a distance of 40 nm from the base of an ideal $500 \times 500 \text{ nm}^2$ gold gammadion for unpolarized (a), right circularly polarized (b) and left circularly polarized (c) light of 550 nm. The ratio between the intensity difference for right- and left-CPL illumination with respect to their sum is presented in (d).

On the basis of these results, we assert that an ideal gammadion does not exhibit any optical activity. So, in principle, this structure should not offer any advantage for chiral biosensing with respect to other forms of 2D achiral plasmonic nanostructures. However, in practice, the simple dissymmetric interaction of only one side of the nanostructures with biomolecule analytes would be enough to break the planarity, thus giving rise to some optical activity at the energies of the plasmonic resonances of the gammadia. This effect will be further enhanced by the inevitable rounding of the gammadia edges.

In the near field, gammadion nanostructures exhibit complex intensity distributions due to the light scattered by the individual arms. Figure 7 shows the normalized near field electric field intensity distribution for an ideal gammadion excited with unpolarized (a), left circularly polarized (LCP) (b) and right circularly polarized (RCP) (c) light of wavelength 550 nm. The near-field interaction between arms of the gammadion enhances the local electric field and the intensity distribution depends strongly on the handedness of the incident radiation. Figure 7(d) shows the normalized difference between electric field intensities for LCP and RCP excitation that corresponds to the element M_{03} of a normalized Mueller matrix. In this near field calculation one can distinguish regions of the gammadion with a clear preference towards LCP or RCP radiation. However, the far field response of the ideal gammadion [Fig. 5(a)] is not sensitive to the handedness of the incoming radiation. This occurs because the distribution of values in Fig. 7(d) averages to zero.

5. Conclusion

In this work we have investigated the origin of the chiroptical effects of a plasmonic nanostructure made of gammadia. A planar, chiral structure cannot exhibit optical activity. However, fabricated nanostructures are not ideal and always have some degree of non-planarity due to rounded edges. Moreover, if a 2D chiral structure is backed by a substrate the mirror symmetry is broken and the ensemble structure-substrate is 3D chiral. Because plasmonic nanostructures can localize and enhance electromagnetic fields, quasi-planar systems such as gold gammadia arrays can exhibit remarkable values of optical activity even if they are very thin “2D” films. Gammadia arrays or, more generally, metamaterials are also prone to exhibit asymmetric transmission of CPL whenever the four-fold symmetry is broken. This effect, totally different from optical activity, arises when there is a planar dissymmetry but it does not require any non-planar

dissymmetry.

Acknowledgments

Yigal Lilach and Michal Eitan are gratefully acknowledged for fabrication of the gammadion arrays. Funding sources: Ministerio de Economía y Competitividad (FIS2012-38244-C02-02 and CTQ2013-47401-C2-1-P), European Commission (Marie Curie IIF Fellowship PIIF-GA-2012-330513, Nanochirality), US National Science Foundation (DMR-1105000) and US National Science Foundation Predoctoral Fellowship (DGE-12342536).